Supplementary Material (ESI) for Chemical Communications

General application of mechanochemistry to templated solid-state reactivity: rapid and solvent-free access to crystalline supermolecules.

Manza B.J. Atkinson, Dejan-Kresimir Bucar, Anatoliy N. Sokolov, Tomislav Friščić, Chanceity Robinson, Mahmood Bilal, Naif G. Sinada, Asher Chevannes and Leonard R. MacGillivray*[a]

Department of Chemistry, University of Iowa

Iowa City, IA 52245-1294 (USA)

Supplementary data

Figure S1. Experiments involving resorcinol (**res**) and *trans*-1,2-bis(4-pyridyl)ethylene (**4,4'-bpe**).

Figure S2. Experiments involving 5-methoxyresorcinol (**5-OMe-res**) and **4,4'-bpe**.

Figure S3. Experiments involving 5-cyanoresorcinol (**5-CN-res**) and **4,4'-bpe**.

Figure S4. Experiments involving 4,6-dichlororesorcinol (**4,6-diCl-res**) and **4,4'-bpe**.

Figure S5. Experiments involving **res** and *trans*-1,2-bis(2-pyridyl)ethylene (**2,2'-bpe**).

Figure S6. Experiments involving 4-chlororesorcinol (**4-Cl-res**) and *trans*-1-(2-pyridyl)-2-(4-pyridyl)ethylene (**2,4'-bpe**).

Figure S7. Experiments involving 1,8-bis(4-pyridyl)naphthalene (**DPN**) and fumaric acid (**fum**).

Figure S8. Experiments involving 2,3-bis(4-methylenethiopyridyl)naphthalene (**2,3-nap**) and **fum**.

Figure S9. ^{1}H-NMR spectrum of ground dry mixture of **res** and **4,4'-bpe** after UV-irradiation.

Figure S10. Cell constants for **(5-CN-res)·(4,4'-bpe)** and **(4,6-diCl-res)·(4,4'-bpe)**.

Fig. S1. Powder X-ray diffraction pattern of (a) simulated pattern from single-crystal structure of **(res)**·(**4,4'-bpe),** (b) ground dry mixture of **res** + **4,4'-bpe** (1 hr), (c) ground dry mixture of **res** + **4,4'-bpe** (45 min), (d) ground dry mixture of **res** + **4,4'-bpe** (30 min), (e) ground dry mixture of **res** + **4,4'-bpe** (15 min), (f) ground dry mixture of **res** + **4,4'-bpe** (3 min), (g) **4,4'-bpe,** (h) **res**.

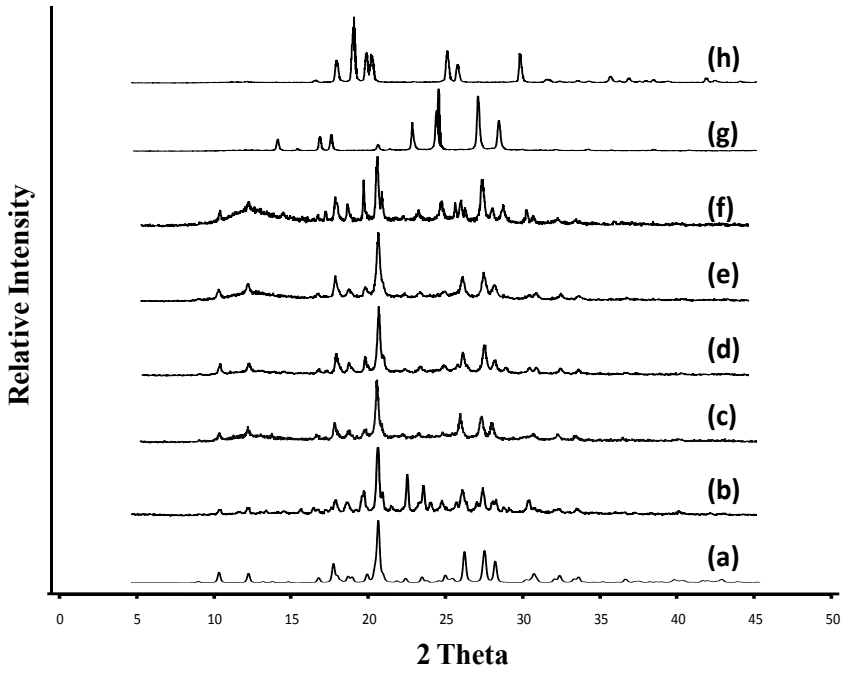

Fig. S2. Powder X-ray diffraction pattern of (a) simulated pattern from single-crystal structure of (**5-OMe-res)·(4,4'-bpe)** (b) ground dry mixture of **5-OMe-res** + **4,4'-bpe** (15 min).

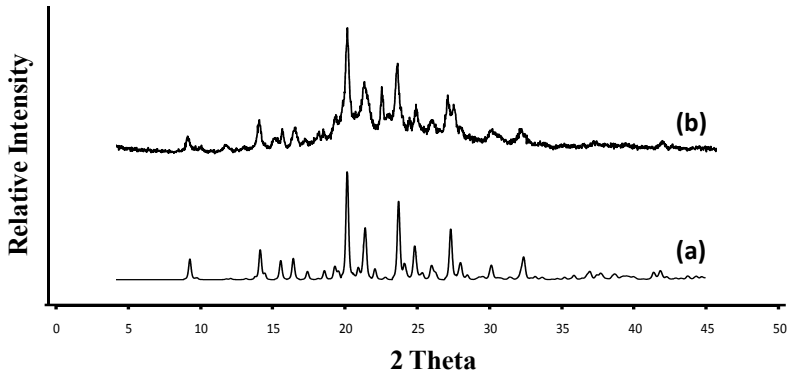

Fig. S3. Powder X-ray diffraction pattern of (a) simulated pattern from single-crystal structure of (**5-CN-res)·(4,4'-bpe)** and (b) ground dry mixture of **5-CN-res** + **4,4'-bpe** (15 min).

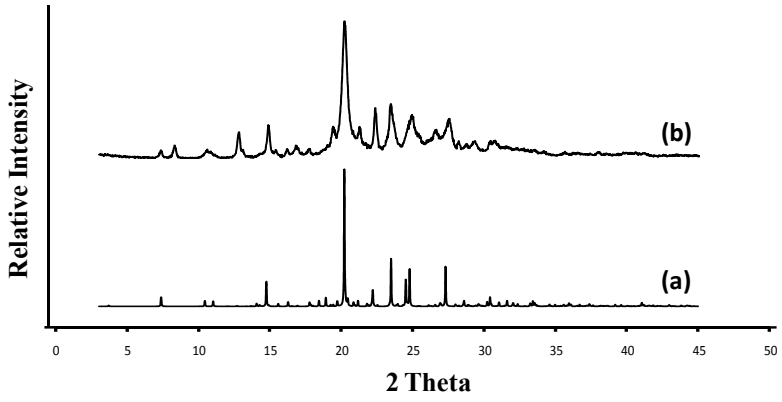

Fig. S4. Powder X-ray diffraction pattern of (a) simulated pattern from single-crystal structure of (**4,6-diCl-res**)·(**4,4'-bpe**) and (b) ground dry mixture of **4,6-diCl-res** + **4,4'-bpe** (15 min).

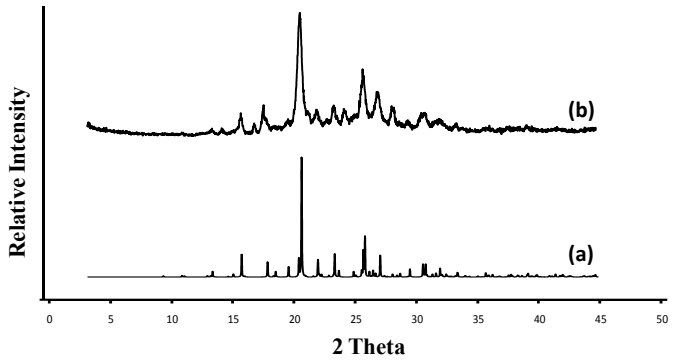

Fig. S5. Powder X-ray diffraction pattern of (a) simulated pattern from single-crystal structure of (**res**)·(**2,2'-bpe)** and (b) ground dry mixture of **res** + **2,2'-bpe** (15 min).

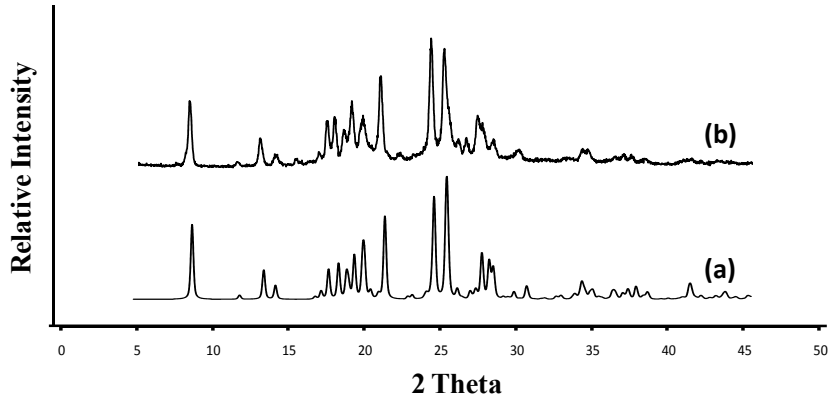

Fig. S6. Powder X-ray diffraction pattern of (a) simulated pattern from single-crystal structure of (**4-Cl-res**)·(**2,4'-bpe)** and (b) ground dry mixture of **4-Cl-res** + **2,4-bpe** (15 min).

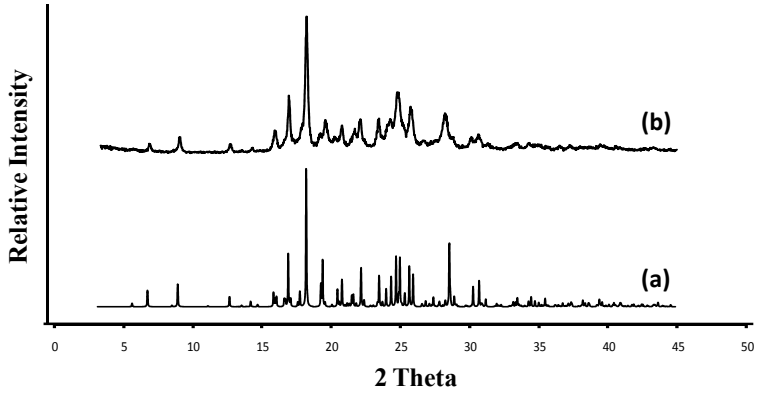

Fig. S7. Powder X-ray diffraction pattern of (a) simulated pattern from single-crystal structure of (**DPN**)·(**fum**), (b) ground dry mixture of **DPN** + **fum** (1hr), (c) ground dry mixture of **DPN** + **fum** with EtOAc (10 min), (d) **fum**, and (e) **DPN**.

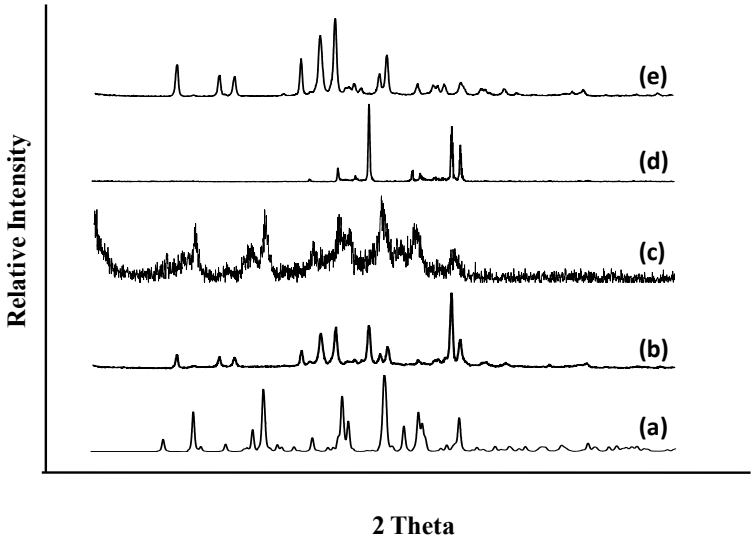

Fig. S8. Powder X-ray diffraction pattern of (a) simulated pattern from single-crystal structure of (**2,3-nap)·(fum)**, (b) ground dry mixture of **2,3-nap** + **fum** (1hr), (c) ground dry mixture of **2,3-nap** + **fum** with EtOAc (10 min), (d) **fum**, and (e) **2,3-nap**.

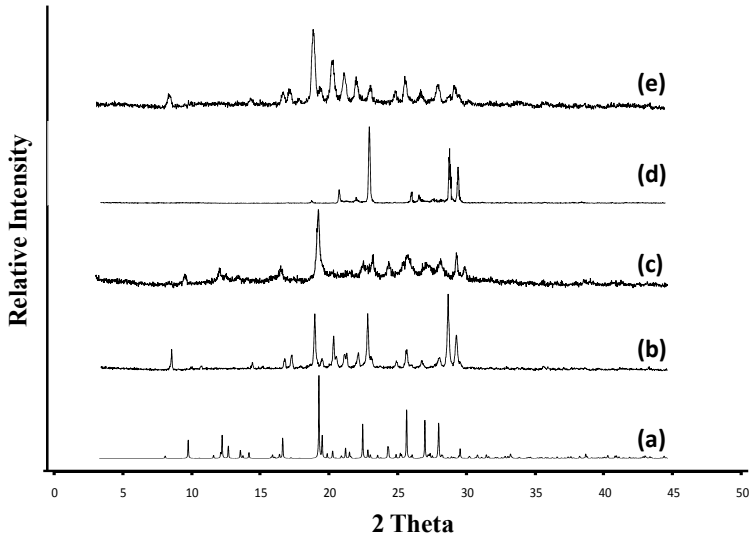

Fig. S9. ^{1}H-NMR spectrum of ground (3 min.) dry mixture of **res** and **4,4-bpe** after UV-irradiation.

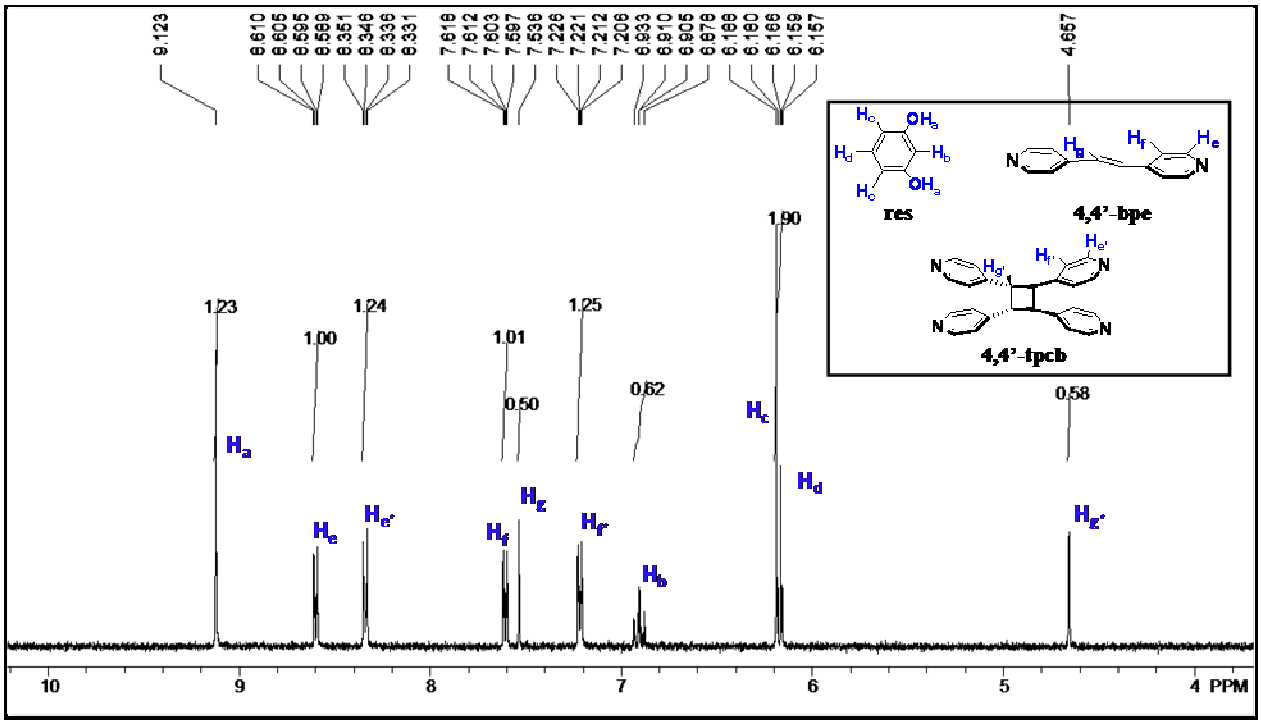

Fig. S10. Cell constants for **(5-CN-res)·(4,4'-bpe)** and **(4,6-diCl-res)·(4,4'-bpe)**.

(5-CN-res)·(4,4'-bpe):

a = 7.643(5)
b = 9.198(5)
c = 24.120(5)
alpha = 85.24(1)
beta = 89.50(1)
gamma = 73.43(1)
space group = P -1

(4,6-diCl-res)·(4,4'-bpe):

a = 8.5991(10)
b = 11.8300(13)
c = 16.6872(18)
beta = 99.119(5)
space group = P 21/n

Structure details will be reported at a later date.